

# Artificial Neural Network for Predicting Hardness of Multistage Solutionized and Artificially Aged LM4 + TiB<sub>2</sub> Composites

D. Srinivas<sup>a</sup>, Gowri Shankar<sup>a\*</sup> , Sathyashankara Sharma<sup>a</sup> , Manjunath Shettar<sup>a</sup> ,

Pavan Hiremath<sup>a</sup>

<sup>a</sup>Manipal Academy of Higher Education, Manipal Institute of Technology, Department of Mechanical and Manufacturing Engineering, Manipal, 576104, Karnataka, India.

Received: October 30, 2021; Revised: December 11, 2021; Accepted: December 14, 2021

Aluminium casting alloy LM4 (EN 1706 AC-45200) composites with TiB<sub>2</sub> (1, 2, and 3 wt.%) as reinforcements were produced using the two-stage stir casting method. OM and SEM study shows uniform and homogeneous reinforcement distribution in LM4 + TiB<sub>2</sub> composites. As-cast composites were subjected to single-stage solution treatment at 520°C for 2 h and multistage solution treatment at 495 and 520°C for 2 and 4 h, followed by hot water quenching at 60°C and aging at 100 and 200°C for different time intervals. The hardness of as-cast and artificially aged composites were compared in both conditions. Compared to as-cast LM4 alloy, 20-45% improvement in hardness was observed for LM4 + TiB<sub>2</sub> as-cast composites. 60-150% improvement in hardness was observed in artificially aged LM4 + 3 wt.% TiB<sub>2</sub> composites when aged at 100 and 200°C during peak aged conditions. TEM images confirmed the presence of primary strengthening solute-rich phases after age hardening treatment such as θ'-Al<sub>2</sub>Cu and θ''-Al<sub>3</sub>Cu, which are responsible for hardness increment. An artificial neural network (ANN) model was created to predict the hardness trend of these composite samples using MATLAB R2021b, and results proved that the ANN model developed can be utilized as an effective tool to predict the hardness of treated composite samples.

**Keywords:** Single-stage solution heat treatment (SSHT), Multistage solution heat treatment (MSHT), Aging treatment, Artificial neural network (ANN), Hardness, LM4 - Aluminium casting alloy (EN 1706 AC-45200).

## 1. Introduction

### 1.1. Basic introduction

Castings made of aluminum-based alloys have played a significant part in the expansion of the aluminium industry. Because of their unique qualities, aluminium alloys have been utilized in the aircraft industry with a substantial substitution of steel components<sup>1,2</sup>. Al-Si alloys are among the various aluminium alloys widely utilized in the production of cylinder heads, pistons, and valve lifters<sup>3</sup>. Hypoeutectic Al-Si alloys have been widely researched and are regarded as good alternatives for automotive components because of their low density, good formability, and outstanding wear resistance<sup>4</sup>. LM4 alloy (hypoeutectic alloy) offers a remarkable blend of strength, low coefficient of thermal expansion at increased temperatures, and great wear resistance<sup>5</sup> and can be used in clutches, tool handles etc<sup>3</sup>. In comparison to other aluminium alloys, LM4 aluminium alloy has higher mechanical strength and greater wear resistance<sup>6</sup>. Mechanical characteristics of Al-Si alloys can be enhanced further by including ceramics particulates<sup>7</sup>. Ceramic particle reinforced aluminium matrix composites are gaining popularity owing to many enhanced characteristics that individual aluminium base alloys cannot provide<sup>8</sup>. Stir casting is a cost-effective

process for producing composites containing discontinuous fibers or particulates<sup>5</sup>. The automobile industry has effectively used aluminium matrix composites (AMCs) in pistons, engine blocks, and other parts<sup>9</sup>. Ceramic particulates do not react with aluminium alloy and have a greater impact on mechanical and tribological characteristics<sup>8</sup>, which can be used as reinforcement particles in various high-temperature applications<sup>6</sup>. TiB<sub>2</sub> reinforced aluminium matrix composites have superior tribological and mechanical characteristics compared to other reinforced AMCs<sup>8</sup>. It is commonly recognized that the obtained effective grain refining is related to the TiB<sub>2</sub> particles' potential heterogeneous nucleation sites and the significant growth limitation effects of the solute Ti (dissolved from Al<sub>3</sub>Ti) for the α-Al crystals<sup>4</sup>. Age hardening heat treatment methods significantly impact the mechanical properties of Al-Si alloys<sup>3</sup>. Heat treatment, particularly solution treatment, causes the trapped gas to expand significantly, forming surficial blisters within large porosities, resulting in weak and dispersed mechanical characteristics<sup>10</sup>. These alloys are often heat treated in two steps to enhance their mechanical properties: i) solution heat treatment, ii) artificial aging. Heating time and heating temperature have been found to influence alloy strength processes such as dissolution of rich phases and Si modification. To avoid incipient melting, conventional solubility temperature must be lower than the

\* e-mail: [gowri.shankarmc@manipal.edu](mailto:gowri.shankarmc@manipal.edu)

melting point of Cu enriched phase; nevertheless, it must be high enough to produce the Cu enriched solid solution phase and Si spheroidization<sup>11</sup>. The type, vol.%, and size of precipitate from supersaturated solid solution during ageing treatments determine the strength of aluminium alloys<sup>12</sup>. Solutionizing time is a critical variable that contributes to the dissolution of Cu phases and improves precipitation of  $\theta''$  and  $\theta'$ -Al<sub>2</sub>Cu during aging<sup>13</sup>.  $\theta''$  and  $\theta'$  precipitates are considered to be responsible for strengthening of the A319 alloy during aging treatment<sup>12,14,15,16</sup>.

### 1.2. Hardness variation in various Al-Si composites

Rajeev et al.<sup>5</sup>, fabricated Al-Si composites reinforced with SiC<sub>p</sub> particulates having an average particle size of 32  $\mu$ m. Al-Si + SiC<sub>p</sub> composites were subjected to age hardening treatment, and results revealed that heat treated composite displayed better hardness (148.3 VHN) when compared to as-cast composite and alloy. Mohapatra et al.<sup>3</sup>, performed homogenization treatment (400, 450, and 500°C for 10 h) on LM4 alloy and calculated hardness at outer, middle, and inner regions of alloy. Results revealed that before homogenization, the outer region exhibited the highest hardness (101 HV) compared to other regions. After homogenization, irrespective of the region, the hardness values dropped (less than the non-homogenized sample). They concluded that hardness could be enhanced by performing artificial aging to the homogenized samples. Shanmugaselvam et al.<sup>17</sup>, fabricated LM4 hybrid composites using nano Al<sub>2</sub>O<sub>3</sub> (1, 1.5, 2.5, 5 wt.%) and micro Mo (0.5 wt.%) as reinforcements. A two-stage stir casting method was used to prepare the composites, and reinforcements were preheated at 800°C for 30 minutes. Nano Al<sub>2</sub>O<sub>3</sub> and micro-Mo formed an oxide layer on the matrix, which restricts the dislocation motion of the particles in the matrix. This phenomenon caused an increase in the hardness of hybrid composite (79 RHF at 5 wt.% Al<sub>2</sub>O<sub>3</sub> + 0.5 wt.% Mo) compared to alloy and other combinations. Mandal et al.<sup>18</sup>, studied the effect of Mg (0-3 wt.%), Sr (0.03 wt.%), and T6 treatment on Al-Si alloy. Results revealed that the modification effect to Mg, Sr, and T6 treatment caused the better distribution of Mg<sub>2</sub>Si and eutectic Si in Al matrix, which showed better mechanical properties comparable to Al-Si + TiB<sub>2</sub> composites. Syukron et al.<sup>7</sup>, fabricated Al-Si + TiB<sub>2</sub> (1.5 wt.%) composite using the stir casting method. Annealing and equal channel angular pressing (ECAP) was performed on alloy and composite. Results revealed that annealing + ECAP showed better hardness (88 VHN) when compared to annealed and as-cast samples. Tabibian et al.<sup>19</sup>, studied the influence of the aging process on lost foam casted (LFC) and die-casted (DC) A319 and A356 + T7 alloys. The results show that softening of A319 is slower than A356; also, A319 (LFC) exhibited the highest hardness value (105 VHN) before and after over-aging compared to other combinations. Medrano-Prieto et al.<sup>11</sup>, studied the behaviour of Al-Si + Ni (up to 2 wt.%) composites before and after T6 treatment. The results concluded that after aging treatment, the effect of Ni is seen, which resulted in the formation of new precipitates that caused an increase in hardness

(142.5 VHN at 2 wt.% Ni addition). Table 1 shows the effect of various heat treatment parameters and reinforcements on the hardness of Al-Si alloys.

### 1.3. Artificial neural network (ANN)

In today's world, to build/manufacture a particular component/product that is to be used in industry, it is important to have complete knowledge of the mechanical properties of the materials used and how they behave during working conditions. Materials behave differently at different temperatures under different loadings. Keeping all the requirements in mind, the components are designed that can withstand any type of condition and loading. At the same time the material must be selected from the lot, which has to meet the required specifications like hardness, tensile strength; if not, it has to be treated to attain the required properties. A lot of time, money, and energy is wasted to test and select materials with the right composition and properties. The alternate solution is the usage of ANN, and here we can predict the properties of materials by giving certain inputs to the model. Usage of ANN is an efficient, less tedious, cheaper, and most reliable method when trained properly. ANN is preferred because it can very well handle nonlinear relations that exist between input and output variables. The working of ANN is clearly explained by Hosein et al.<sup>22</sup>.

Nwobi-Okoye et al.<sup>23</sup>, used both ANN and ANFIS (Adaptive Neuro-Fuzzy Inference System) for modeling and optimization for the age hardening process. A356/cow horn composite was prepared, and aging data was collected to train, validate and test models. Temperature, wt.%, and time were used as inputs. From their work, they concluded that ANN is proven to be more effective than ANFIS. Results proved that the ANN method could effectively be used to predict composites' properties. Van Nguyen et al.<sup>24</sup>, used the ANN model to predict hardness change in wood during heat treatment. Temperature, time, and wood species were used as input variables, Levenberg-Marquardt backpropagation is used as a training algorithm. Four neurons were used in the hidden layer and wood hardness as the output variable. From the results, it was clear that ANN can be used to predict wood hardness at different heat treatment parameters; this one can create a heat treatment program that will give the required hardness without needing to conduct experiments. Liu et al.<sup>25</sup>, used ANN to study the co-relation between silicide and fracture toughness of Nb-Si alloys. They used  $\gamma$ -Nb<sub>5</sub>Si<sub>3</sub> size, Nb<sub>5</sub>Si<sub>3</sub> size, Nb<sub>5</sub>Si<sub>3</sub> shape, Nb<sub>ss</sub> morphology, volume fraction as input variables, traingdm training algorithm is used. Experiments were conducted to train, validate and test the model. From the results, they concluded that ANN established an effective relationship between microstructure and fracture toughness, cause and effect can be easily studied by the use ANN model. Optimization is also done successfully. LouieFrango et al.<sup>26</sup>, prepared nickel-CBN composite coatings using electrodeposition techniques. ANN predicted hardness values were compared with experimental hardness values. Three input variables were used in this study (pH, current density, temperature), to train the model feed-forward backpropagation algorithm

**Table 1.** Effect of various heat treatment parameters and reinforcements on the hardness of Al-Si alloys.

S. No	Matrix	Reinforcement	Type of heat treatment used	Solution heat treatment parameters		Aging parameters		Highest hardness value @ best conditions	Reference
				Temp (°C)	Time (h)	Temp (°C)	Time (h)		
1	Al-Si alloy	SiC <sub>p</sub>	Age hardening	500	6	190	12	148.3 VHN @ 15 wt.% SiC <sub>p</sub>	Rajeev et al. <sup>5</sup>
2	LM4	-	Homogenized	400, 450 and 500	10	-	-	101 HV (for non-homogenized sample)	Mohapatra et al. <sup>3</sup>
3	LM4	-	Multi axial forging	-	-	-	-	74 VHN for 5 passes	Sajjan et al. <sup>20</sup>
4	LM4	Al <sub>2</sub> O <sub>3</sub> and Mo	-	-	-	-	-	79 RHF at 5 wt.% Al <sub>2</sub> O <sub>3</sub> + 0.5 wt.% Mo	Shanmugaselvam et al. <sup>17</sup>
5	Al-5.7Si-2Cu-0.3 Mg	-	Thixoformed + T6	485	12	190	10	80 HRB (thixoformed +T6)	Abdelgnei et al. <sup>2</sup>
6	Al-Si	Mg, Sr (modifiers)	T6	540	6	155	8	Comparable to that of Al-Si + TiB <sub>2</sub> composites	Mandal et al. <sup>18</sup>
7	Al-Si	TiB <sub>2</sub>	Annealing and ECAP	540	8	-	-	88 VHN (Annealing + ECAP)	Syukron et al. <sup>7</sup>
8	A319	-	Aging	-	-	150, 200, 250	3, 6, 9, 30, 60, 90, 200, 300 and 500	105 VHN (A319 LFC)	Tabibian et al. <sup>19</sup>
9	A319	Ni (modifier)	T6	495	5 and 7	170	0.5, 4, 6, 10, 96	142.5 VHN at 2 wt.% Ni	Medrano-Prieto et al. <sup>11</sup>
10	A319 and A356	-	Two step solution annealing	500 and 545	4 and 10	200	Up to 600	Improved hardness	Farkoosh et al. <sup>21</sup>

is used. Results showed that ANN predicted experimental hardness results with an error of 0.06141%. Xia et al.<sup>27</sup>, studied the compositional effect on hardness and corrosion for magnesium alloys. ANN was used to predict the hardness and corrosion values, and alloying elements were given as input variables. From the results, it is evident that ANN accurately predicted the hardness and corrosion values. Amirjan et al.<sup>28</sup>, prepared Cu-Al<sub>2</sub>O<sub>3</sub> composites using the powder metallurgy method. Experiments were conducted to calculate electrical conductivity and hardness. ANN prediction is made with sigmoid activation function and backpropagation training algorithm. Predicted values are on par with experimental values with an error of 5 and 3% for hardness and electrical conductivity. Taghizadeh *et al.*<sup>29</sup>, predicted hardness drop in tempered and quenched AISI 1045 steel with the help of ANN. Tempering temperature and tempering time were used as input variables, and fermi's transfer function is used for hidden and output layers. From results it was evident

that ANN correctly predicted a drop in hardness values. Meyveci et al.<sup>30</sup>, predicted the hardness of age hardened A2024 and A6063 alloys by using ANN. Temperature and time were taken as input variables, two hidden layers and one output variable. Based on the findings, they concluded that experimental and predicted values are in reasonable agreement. Based on the thorough literature review, it was observed that limited research work was carried out on MSHT to improve the mechanical properties of TiB<sub>2</sub> reinforced composites. An attempt is made to know the impact of MSHT on LM4 + TiB<sub>2</sub> composites as compared to SSHT age hardening treatment. To predict mechanical properties of alloys/composites, only three or four input variables are considered, which provided minimum error prediction in their respective work, but some major parameters (as input variables) were neglected, which are very important for property variation. Therefore, the present research work mainly focuses on the importance of ANN model to

predict hardness improvement in composite samples using MATLAB R2021b.

## 2. Material and Experimental Procedure

### 2.1. Preparation of LM4 + TiB<sub>2</sub> composites

In the present investigation, LM4 + TiB<sub>2</sub> (1, 2, and 3 wt.%) composites were prepared using a two-stage stir casting technique. LM4 alloy was procured from Laxmi metal exchange, Coimbatore, and the chemical composition is shown in Table 2. TiB<sub>2</sub> particulates having an average particle size of 6.765 μm were procured from NANOCHEMAZONE INC, Canada. To prepare LM4 composite with TiB<sub>2</sub> as reinforcement, LM4 alloy is heated to a melting temperature of 780°C in 2 kg crucible. TiB<sub>2</sub> powder is preheated at 350°C for about 30 min before adding to the molten alloy. Before adding reinforcement, molten alloy is stirred at 400 rpm for 5 min, then preheated reinforcement is added, and stirring is done at 400 rpm for 10 min. Melt is poured into preheated molds (500°C for 1 h) and allowed to solidify. The entire stir casting process and cast composites used for the present investigation is shown in Figure 1a, b. Optical Microscope (OM) and Scanning Electron Microscope (SEM) images were collected to confirm the uniform reinforcement distribution of reinforcement particulates in the matrix alloy. The as-cast samples were cut for hardness measurement to perform single-stage solution heat treatment (SSHT) and multistage heat treatment (MSHT). Transmission Electron

Microscope (TEM) analysis was performed to investigate the strengthening mechanism and phase identification in peak aged samples for both SSHT and MSHT.

### 2.2. Age hardening treatment and hardness measurement

Composite samples were divided into four batches. The first batch was subjected to SSHT, where specimens were soaked at 520°C for 2 h, followed by hot water quenching at 60°C and then artificial aging at 100°C. The second batch was subjected to SSHT and artificial aging at 200°C. The third batch was subjected to MSHT, where samples were soaked at 495 and 520°C for 2 and 4 h, followed by hot water quenching at 60°C and artificial aging at 100°C. The fourth batch was subjected to MSHT and artificial aging at 200°C. Artificial aging is performed at these two temperatures (100 and 200°C) for various durations of time. As per the literature<sup>31</sup>, when A319 alloy is subjected to SSHT (495°C for 8 h, followed by 60°C water quenching), modification of Si and dissolving of Cu were not observed, whereas when subjected to two-stage SHT (495°C for 2 h and 520°C for 4 h) it gave better results. A schematic diagram of the heat treatment carried out in the present work is shown in Figure 2. A Vickers Hardness test was performed at room temperature, with an average of at least five indentations considered. Hardness measurements were done using MATZUSAWA MICRO VICKERS HARDNESS TESTER, MODEL-MMT X 7A with 200gmf load & 15 seconds dwell time. The hardness test specimens were suitably polished to achieve a flat

**Table 2.** Chemical composition of LM4 alloy.

Material	Si	Fe	Cu	Mn	Ni	Ti	Sn	Mg	Al
wt.% (Actual)	5.925	0.641	2.476	0.121	0.03	0.045	0.045	0.176	Bal.
wt.% (Actual)	4-6	0-0.8	2-4	0.2-0.6	0-0.3	0-0.2	0-0.1	0-0.2	Bal.

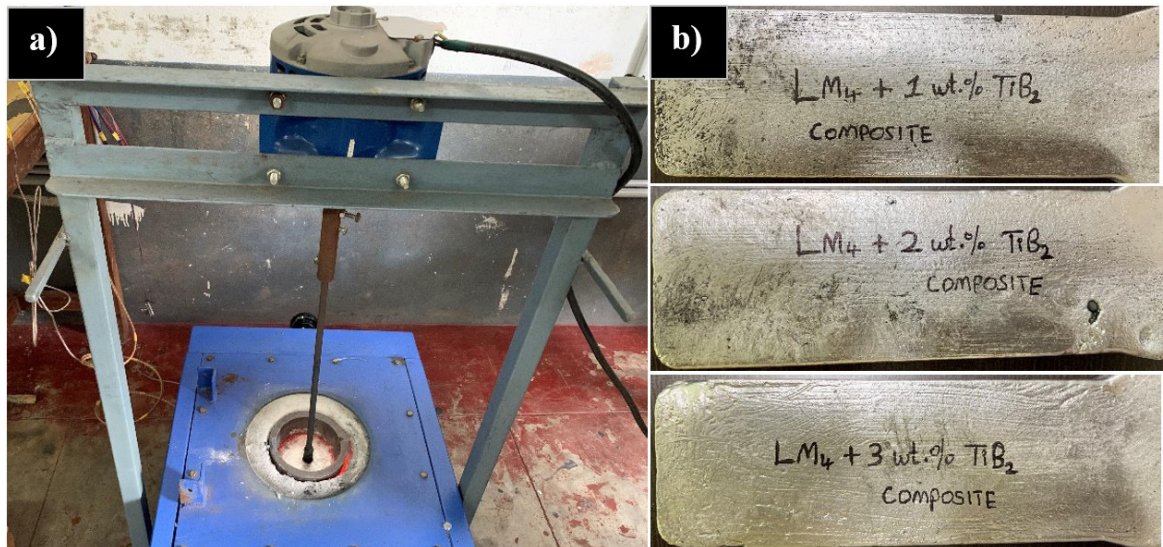


**Figure 1.** (a) Stir casting setup used for present investigation, (b) Cast composites used in present work.



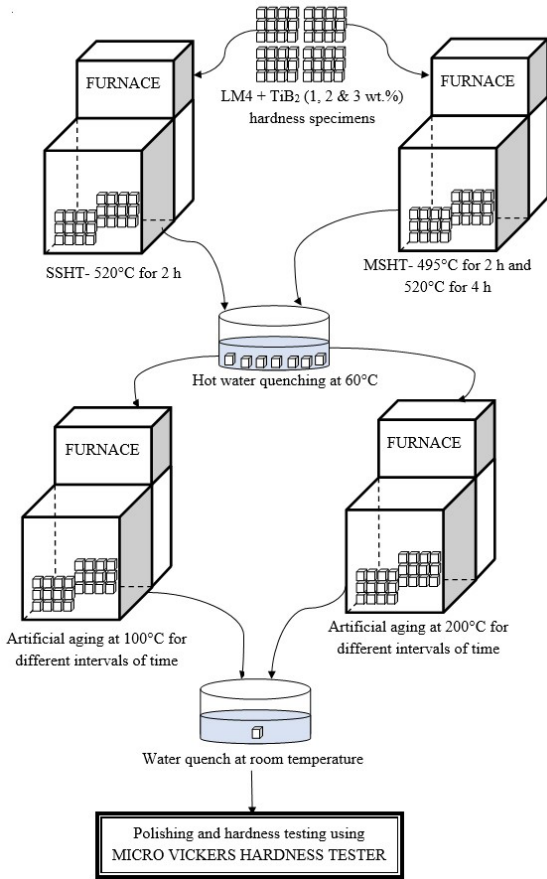


**Figure 2.** Schematic diagram of the age hardening treatment process carried out in present work.

surface. A rotating disc polishing device with a velvet cloth saturated with diamond paste and liquid diamond spray was utilized for fine polishing. Hardness levels are taken at 30/60 minute intervals to determine the peak aging duration for that temperature. Before the hardness test, the surface is polished to eliminate any oxide layer or contaminants that may have formed during the heat treatment process.

### 2.3. ANN model

ANN consists of input, output, and hidden layers which are connected to each other. The number of input variables contributes to the number of input neurons and, similarly in the case of output variables. In our case, we have 17 input variables (input neurons) and one output variable (output neuron), as shown in Figure 3. There are additional hidden layers between the input and output layers. Neurons with certain weight factors are linked to neurons in other layers. This weight determines the value of neurons' output, which is then passed on to the succeeding layers. These functions available in ANN will be chosen depending on the problem's complexity, the number of nodes, and weights. The total data set is randomly split into two parts: training and validation. The training set is used to train the model, while the validation set is used to validate it. Validation

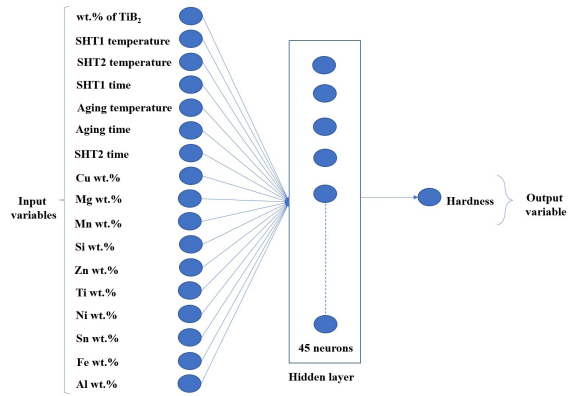


**Figure 3.** Structure of ANN model used in present work.

error can be seen when the network is trained beyond a certain limit (overtrained) with the training data. In such cases, the data with the least amount of validation error is presented as a result. The backpropagation algorithm (BP) is a commonly used learning algorithm for prediction problems. The Levenberg-Marquardt (LM) algorithm is frequently used to solve nonlinear equations. Most of the time trial and error method is used to determine the number of hidden layers in an ANN model<sup>32</sup>, which is time-consuming. By using the thumb rule (Equation 1)<sup>33</sup> number of neurons for the hidden layer were selected, and the prediction was performed using MATLAB R2021b, where  $H_n$  is the number of hidden neurons,  $M$ ,  $N$  are the number of input and output variables and  $T_n$  is the number of total training data. The structure of the ANN model with input, output variables, and the number of hidden neurons is shown in Figure 3.

$$H_n = \frac{M + N}{2} + \sqrt{T_n} \quad (1)$$

## 3. Results and Discussion

### 3.1. Distribution of reinforcements

Superior mechanical properties need uniform distribution of reinforcements in the metal matrix. Microstructural investigation and analysis will provide some insight into the composite's quality. The two main factors examined during the fabrication of particulate composites are homogeneous particle distribution in the liquid melt and the prevention of particle segregation/agglomeration during pouring and solidification. An optical microscope is used to ensure uniform dispersion of TiB<sub>2</sub> reinforcement in the matrix alloy. Figure 4a-d depicts optical micrographs of LM4 alloy and LM4 + TiB<sub>2</sub> (1, 2, and 3 wt.%) composites. The micrographs show that the TiB<sub>2</sub> particles are distributed uniformly in the LM4 alloy matrix with no reinforcement agglomeration. The dark spots are identified as discrete TiB<sub>2</sub> particles embedded in an LM4 matrix. Microstructure did not indicate the presence of any blowholes. This is due to efficient stirring action and the adoption of optimal process parameters during AMC fabrication. As shown in Figure 5a, b, SEM images of LM4+3 wt.% TiB<sub>2</sub> and EDAX analysis (Figure 5c) confirm

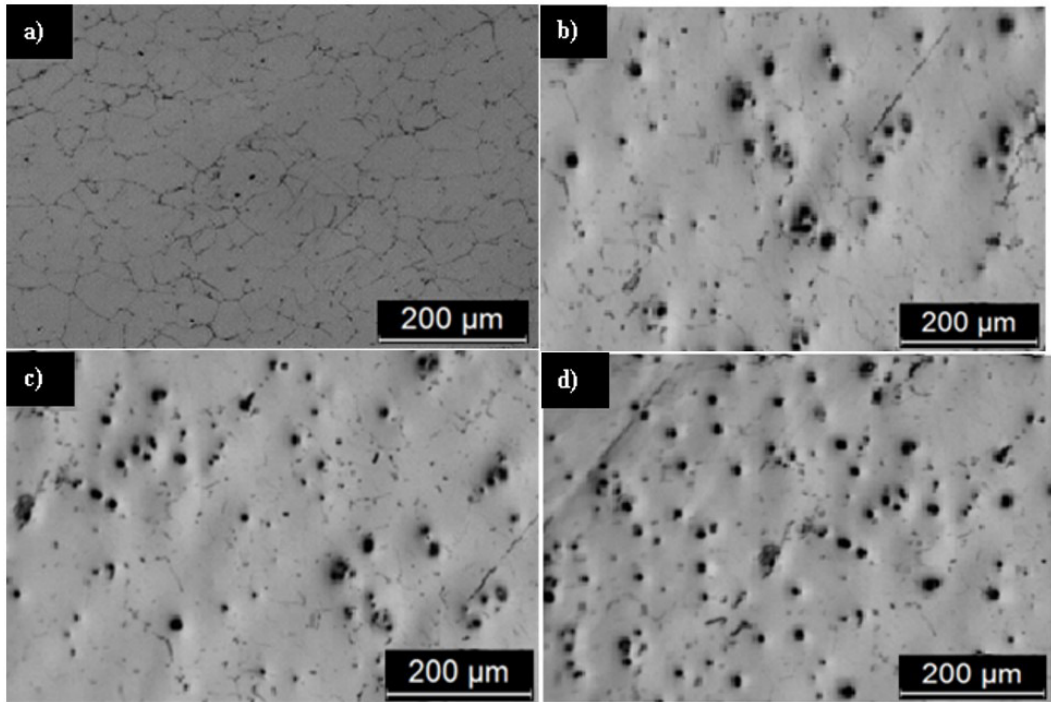


Figure 4. Optical microstructures of (a) LM4 alloy, (b) LM4 + 1 wt.% TiB<sub>2</sub>, (c) LM4 + 2 wt.% TiB<sub>2</sub>, (d) LM4 + 3 wt.% TiB<sub>2</sub>

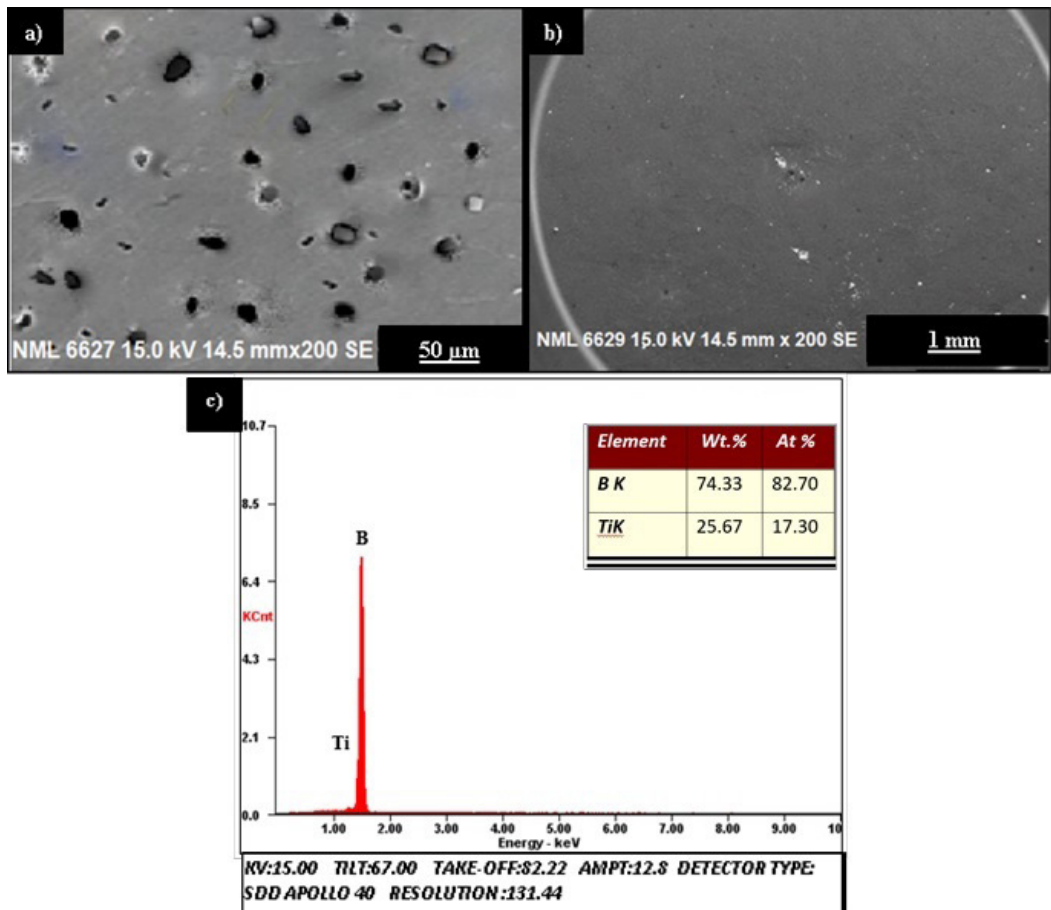


Figure 5. (a, b) SEM images of LM4 + 3 wt.% TiB<sub>2</sub> composite sample and (c) EDAX of LM4 + 3 wt.% TiB<sub>2</sub> composite sample.

the uniform distribution and presence of TiB<sub>2</sub> reinforcement powder in the matrix alloy.

### 3.2. Hardness measurement of the age hardened samples

Both as-cast and age hardened samples of LM4 alloy and LM4 + TiB<sub>2</sub> (1, 2, and 3 wt.%) composites are subjected to hardness measurement (VHN). A total of 96 samples were examined for hardness, with each sample tested five times and the mean result utilized. Hardness is found to increase gradually with aging time for both the LM4 alloy and its composites. It reaches to peak hardness value followed by over-aging, which results in the decrease of hardness. The duration to reach peak aging is found to reduce with an increase in wt.% of TiB<sub>2</sub> (1, 2, and 3 wt.%) reinforced composites at 100 and 200°C aging temperatures. As-cast LM4 alloy displayed 70 VHN, whereas LM4 + TiB<sub>2</sub> (1, 2, and 3 wt.%) as-cast composites show 89, 95, and 103 VHN, respectively. The increase in hardness of as-cast composites is mainly due to the presence of hard dispersoids, which positively contribute to the hardness of the composites. Because of the thermal mismatch between alloy and reinforcement, increased dislocation density can be seen during solidification as the wt.% of reinforcement increases. As a result, the microstructure and mechanical properties of the composites are affected by high internal stresses and mismatch strain. The matrix deforms plastically to meet the reinforcement particles' smaller volume expansion, resulting in greater dislocation density. Increased dislocation density leads to increased resistance to plastic deformation and contributes to an increase in composite hardness. The current experimental results are consistent with the reported research findings<sup>34-36</sup>. Figures 6 and 7 show the peak hardness values of both SSHT and MSHT for different aging temperatures at 100 and 200°C for both LM4 alloy and LM4 + TiB<sub>2</sub> composites. Compared to as-cast LM4 alloy, 80-150% increase in hardness was observed when aged at 100°C and 65-120% increase in hardness was observed at 200°C during SSHT and MSHT, respectively. Aging helps to improve the hardness by precipitating solute-rich phases from supersaturated solid solution<sup>34</sup>. Lower ageing temperature (100°C) have higher hardness than higher aging temperatures (200°C); however, the time necessary to attain peak hardness is longer at 100°C, which can be explained by aging kinetics<sup>37</sup>. MSHT specimens have a greater hardness than SSHT specimens. This enhancement is mainly owing to the full homogenization of secondary solute-rich phases at ambient temperature throughout the multistage solutionizing process. These phases will precipitate as fine precipitates inside the matrix during ageing, resulting in a significant improvement in hardness during MSHT.

Figure 8 shows the TEM image of SSHT LM4 + 3 wt.% TiB<sub>2</sub> sample aged at 100°C under different magnification. From Figure 8b, we can see the presence of  $\theta'$ -Al<sub>2</sub>Cu and  $\theta''$ -Al<sub>3</sub>Cu (primary strengthening phases), which are responsible for peak aging<sup>12</sup>. Similarly, Figure 9 also shows the TEM image of MSHT LM4 + 3 wt.% TiB<sub>2</sub> sample aged at 100°C under different magnification. Also, Figure 9b confirms the presence of  $\theta'$ -Al<sub>2</sub>Cu and  $\theta''$ -Al<sub>3</sub>Cu (primary strengthening phases). After age hardening treatment, the peak aged sample

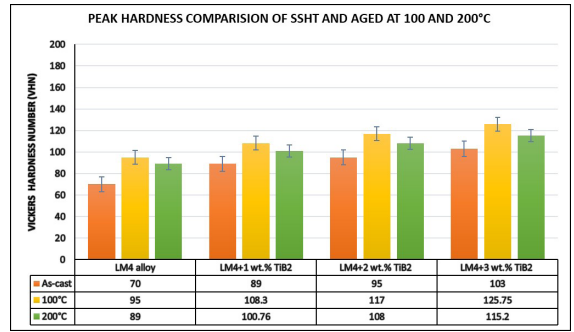


Figure 6. Peak hardness values of LM4 alloy and LM4 + TiB<sub>2</sub> composites in as-cast and different aging conditions during SSHT.

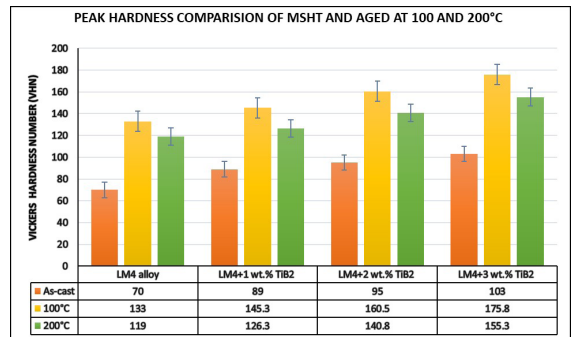
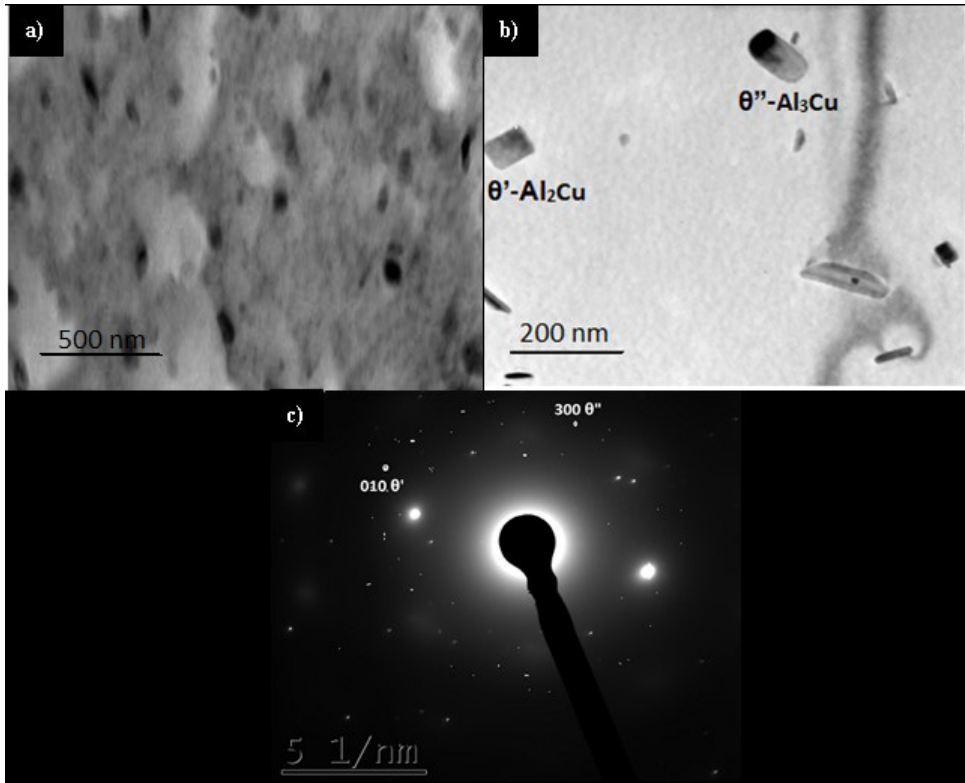


Figure 7. Peak hardness values of LM4 alloy and LM4 + TiB<sub>2</sub> composites in as-cast and different aging conditions during MSHT.

shows the presence of  $\theta''$ -Al<sub>3</sub>Cu and  $\theta'$ -Al<sub>2</sub>Cu metastable phases, that are responsible for substantial improvement in hardness as compared to as-cast LM4 alloy, whereas MSHT sample shows more number of precipitates as compared to SSHT samples<sup>13,15</sup>. Figures 8c and 9c show selection area diffraction pattern (SADP), which clearly indicates that MSHT samples aged at 100°C have more number of precipitates than SSHT samples aged at 100°C, which resulted in higher hardness of MSHT samples.

### 3.3. Prediction of hardness using ANN

In this study, the prediction of the hardness of LM4 + TiB<sub>2</sub> composites (both single and multistage solutionized and aged) was performed. As experimental results, the mean hardness values of 96 samples were used. By comparing the experimental and prediction results, the model worked fine and was able to predict the hardness values to high-level accuracy. Comparison of hardness values of experimental and that predicted by ANN can be seen in Figure 10. The maximum error obtained was noted to be 4%, and the average error is noted to be 1%. Figure 11 depicts the results displayed against the best fit line. R (coefficient of correlation) values for training, validation, test, and overall data are shown in Figure 11. An additional test was also performed with different data set containing mean hardness values of 18 additional samples, and the graph against the best fit



**Figure 8.** TEM images (a, b) of SSHT along with SADP (c) of LM4 + TiB<sub>2</sub> composite aged at 100°C shows presence of θ'' phase - Al<sub>3</sub>Cu (rod shape) and θ' phase - Al<sub>2</sub>Cu (plate shape).

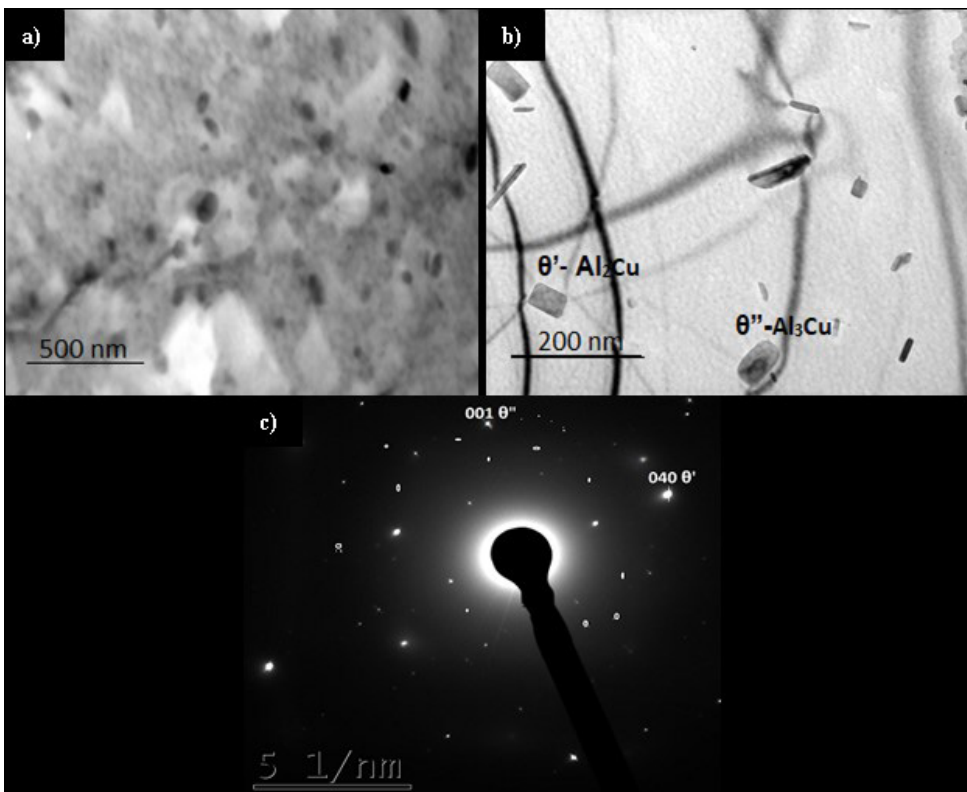


**Figure 9.** TEM photographs (a, b) of MSHT along with SADP (c) of LM4 + TiB<sub>2</sub> composite aged at 100°C shows presence of θ'' phase - Al<sub>3</sub>Cu (rod shape) and θ' phase - Al<sub>2</sub>Cu (plate shape).



having  $R = 0.96384$  is shown in Figure 12. As a result, the ANN precisely predicts the data recorded in the experiment.

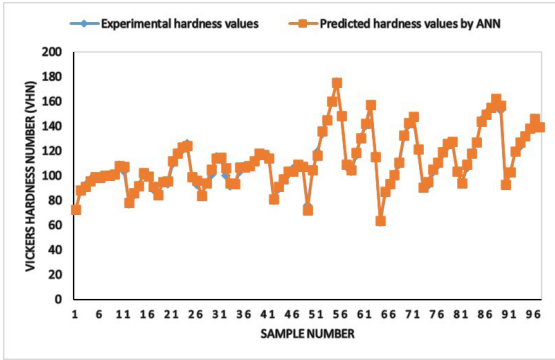


**Figure 10.** Hardness values comparison between experiment and prediction.

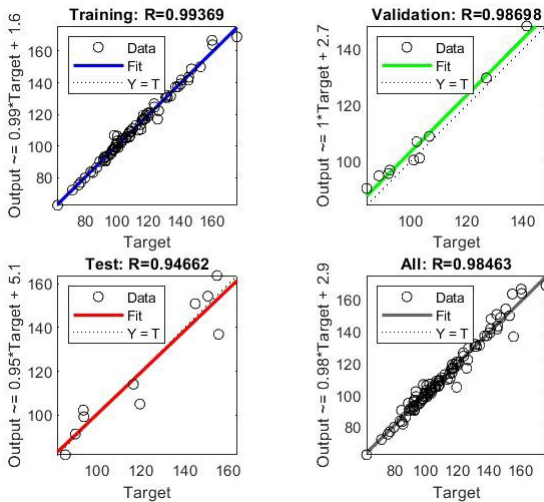


**Figure 11.** Regression analysis with training, testing, validation and all data sets.

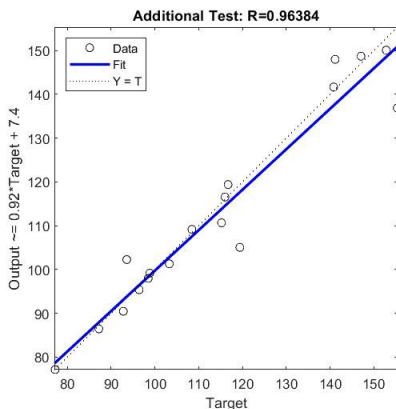


**Figure 12.** Regression analysis of additional test data.

## 4. Conclusions

In the present study, hardness prediction of multistage solutionized and aged LM4 + TiB<sub>2</sub> composites fabricated using a two-stage stir casting method was made. Results led to the following conclusions:

- In preparation of composites, two-stage stir casting is proved to be the best one as all the composites with 1, 2, and 3 wt.% TiB<sub>2</sub> exhibited uniform distribution of reinforcement particles, which is clear from the optical microscope images.
- SEM and EDAX confirmed the presence and uniform distribution of TiB<sub>2</sub> reinforcement powder in LM4 + TiB<sub>2</sub> samples.
- The hardness results show that with an increase in wt.% of TiB<sub>2</sub>, the hardness has increased, and MSHT samples aged at 100°C with 3 wt.% TiB<sub>2</sub> exhibited the highest hardness values when compared to other samples. Aging at 100°C gave better hardness results than aging at 200°C.
- Compared to as-cast LM4 alloy, 80-150% increase in hardness was observed when aged at 100°C, and 65-120% increase in hardness was observed at 200°C during SSHT and MSHT, respectively.
- TEM images confirmed the presence of  $\theta'$ -Al<sub>2</sub>Cu and  $\theta''$ -Al<sub>3</sub>Cu primary strengthening phases after age hardening treatment which are responsible for hardness increment. Also, more number of precipitates were found in MSHT samples when compared to SSHT samples.
- The ANN is a powerful technique for predicting composite properties. Design and manufacturing teams can use predicted values of hardness under specified conditions and prescribed materials as a cost-saving factor in the process. ANN predicted the hardness with an average error of 1%.

## 5. References

1. Nascimento FC, Paresque MCC, De Castro JA, Jácome PAD, Garcia A, Ferreira IL. Application of computational thermodynamics to the determination of thermophysical properties as a function of temperature for multicomponent Al-based alloys. *Thermochim Acta.* 2015;619:1-7.
2. Abdelgnei MA, Omar MZ, Ghazali MJ, Mohammed MN, Rashid B. Dry sliding wear behaviour of thixoformed Al-5.7Si-2Cu-0.3 Mg alloys at high temperatures using taguchi method. *Wear.* 2020;442-443:203134.
3. Mohapatra S, Ilangovan S, Shanmugasundaram A. Effect of homogenization temperature on mechanical and tribological properties of LM4 cast alloy. *Mater Today Proc.* 2020;38:2617-23.
4. Li Q, Qiu F, Dong B-X, Gao X, Shu S-L, Yang H-Y, Jiang Q-C. Processing, multiscale microstructure refinement and mechanical property enhancement of hypoeutectic Al-Si alloys via in situ bimodal-sized TiB<sub>2</sub> particles. *Mater Sci Eng A.* 2020;777:139081.
5. Rajeev VR, Dwivedi DK, Jain SC. Dry reciprocating wear of Al-Si-SiC<sub>p</sub> composites: a statistical analysis. *Tribol Int.* 2010;43(8):1532-41.
6. Sachit TS, Mohan N, Suresh R, Prasad MA. Optimization of dry sliding wear behavior of aluminum LM4-Ta/NbC nano composite using Taguchi technique. *Mater Today Proc.* 2019;27:1977-83.

7. Syukron M, Ojima M, Seman AA, Hussain Z, Koseki T. Mechanical properties of 1.5wt.% TiB<sub>2</sub>-added hypoeutectic Al-Mg-Si alloys processed by equal channel angular pressing. *Procedia Chem.* 2016;19:106-12.
8. Poria S, Sahoo P, Sutradhar G. Design of experiments analysis of wear behavior of stir cast Al-TiB<sub>2</sub> composite in lubricated condition. *Mater Today Proc.* 2018;5(2):5221-8.
9. Gavel A, Poria S, Sahoo P. Design of experiments analysis of abrasive friction behavior of Al-TiB<sub>2</sub> composites. *Mater Today Proc.* 2019;19:218-22.
10. Zhu X, Dong X, Blake P, Ji S. Improvement in as-cast strength of high pressure die-cast Al-Si-Cu-Mg alloys by synergistic effect of Q-Al<sub>5</sub>Cu<sub>2</sub>Mg<sub>8</sub>Si<sub>6</sub> and θ-Al<sub>2</sub>Cu phases. *Mater Sci Eng A.* 2021;802:140612.
11. Medrano-Prieto HM, Garay-Reyes CG, Gómez-Esparza CD, Estrada-Guel I, Aguilar-Santillan J, Maldonado-Orozco MC, et al. Effect of nickel addition and solution treatment time on microstructure and hardness of Al-Si-Cu aged alloys. *Mater Charact.* 2016;120:168-74.
12. Wiengmoon A, Pearce JTH, Chairuangsi T, Isoda S, Saito H, Kurata H. HRTEM and HAADF-STEM of precipitates at peak ageing of cast A319 aluminium alloy. *Micron.* 2013;45:32-6.
13. Medrano-Prieto HM, Garay-Reyes CG, Gómez-Esparza CD, Aguilar-Santillan J, Maldonado-Orozco MC, Martínez-Sánchez R. Evolution of microstructure in Al-Si-Cu system modified with a transition element addition and its effect on hardness. *Mater Res.* 2016;19:59-66.
14. Ovono Ovono D, Guillot I, Massinon D. Determination of the activation energy in a cast aluminium alloy by TEM and DSC. *J Alloys Compd.* 2007;432(1-2):241-6.
15. Hwang JY, Banerjee R, Doty HW, Kaufman MJ. The effect of Mg on the structure and properties of Type 319 aluminum casting alloys. *Acta Mater.* 2009;57(4):1308-17.
16. Yang H, Ji S, Yang W, Wang Y, Fan Z. Effect of Mg level on the microstructure and mechanical properties of die-cast Al-Si-Cu alloys. *Mater Sci Eng A.* 2015;642:340-50.
17. Shanmugaselvam P, Yogaraj JNR, Sivaraj S, Jayakrishnan N. Fabrication and evaluation of tribological behaviour and hardness of aluminium-LM4 reinforced with nano alumina and micro Mo. *Mater Today Proc.* 2021;3(2):844-8.
18. Mandal A, Chippa N, Jayasankar K, Mukherjee PS. Effect of high magnesium content on microstructure of Al-7Si alloy. *Mater Lett.* 2014;117:168-70.
19. Tabibian S, Charkaluk E, Constantinescu A, Guillemot G, Szymka F. Influence of process-induced microstructure on hardness of two Al-Si alloys. *Mater Sci Eng A.* 2015;646:190-200.
20. Sajjan SS, Kulkarni MV, Ramesh S, Sharath PC, Kumar V, Rajole S. Effect of mechanical properties on multi axially forged LM4 aluminium alloy. *Mater Today Proc.* 2020;24:1462-7.
21. Farkoosh AR, Javidani M, Hoseini M, Larouche D, Pegguleryuz M. Phase formation in as-solidified and heat-treated Al-Si-Cu-Mg-Ni alloys: thermodynamic assessment and experimental investigation for alloy design. *J Alloys Compd.* 2013;551:596-606.
22. Sadati H, Alizadeh J, Ghajar R. Application of artificial neural networks in the estimation of mechanical properties of materials. In: Suzuki K, editor. *Artificial Neural Networks - Industrial and Control Engineering Applications.* London: IntechOpen Limited; 2011.
23. Nwobi-Okoye CC, Ochieze BQ, Okiy S. Multi-objective optimization and modeling of age hardening process using ANN, ANFIS and genetic algorithm: results from aluminum alloy A356/cow horn particulate composite. *J Mater Res Technol.* 2019;8(3):3054-75.
24. Van Nguyen TH, Nguyen TT, Ji X, Lanh Do KT, Guo M. Using artificial neural networks (ANN) for modeling predicting hardness change of wood during heat treatment. *IOP Conf Ser Mater Sci Eng.* 2018;394(3):032044.
25. Liu G, Jia L, Kong B, Guan K, Zhang H. Artificial neural network application to study quantitative relationship between silicide and fracture toughness of Nb-Si alloys. *Mater Des.* 2017;129:210-8.
26. LouieFrango T, Ramanathan K, RameshBapu GNK, Marimuthu P. Artificial neural network (ANN) modeling for predicting hardness of Ni-Cbn composite coatings. *Int J Adv Engg Tech.* 2016;7(2):1234-37.
27. Xia X, Nie JF, Davies CHJ, Tang WN, Xu SW, Birbilis N. An artificial neural network for predicting corrosion rate and hardness of magnesium alloys. *Mater Des.* 2016;90:1034-43.
28. Amirjan M, Khorsand H, Siadati MH, Eslami Farsani R. Artificial neural network prediction of Cu-Al<sub>2</sub>O<sub>3</sub> composite properties prepared by powder metallurgy method. *J Mater Res Technol.* 2013;2(4):351-5.
29. Taghizadeh S, Safarian A, Jalali S, Salimiasl A. Developing a model for hardness prediction in water-quenched and tempered AISI 1045 steel through an artificial neural network. *Mater Des.* 2013;51:530-5.
30. Meyveci A, Karacan I, Durmuş H, Çaligülü U. Artificial neural network (ANN) approach to hardness prediction of aged aluminium 2024 and 6063 Alloys. *Mater Test.* 2012;54(1):36-40.
31. Sokolowski JH, Djurdjevic MB, Kierkus CA, Northwood DO. Improvement of 319 aluminum alloy casting durability by high temperature solution treatment. *J Mater Process Technol.* 2001;109(1-2):174-80.
32. Shetty SP, Nayak S, Kumar S, Vasudeva Karanth K. Thermo-hydraulic performance prediction of a solar air heater with circular perforated absorber plate using Artificial neural network. *Therm Sci Eng Prog.* 2021;23:100886.
33. Ghrilahre HK, Chandrakar P, Ahmad A. A comprehensive review on performance prediction of solar air heaters using artificial neural network. Berlin: Springer Berlin Heidelberg; 2019. no. 0123456789.
34. Gowrishankar MC, Hiremath P, Shettar M, Sharma S, Satish Rao U. Experimental validity on the casting characteristics of stir cast aluminium composites. *J Mater Res Technol.* 2020;9(3):3340-7.
35. Shettar M, Hiremath P, Shankar G, Kini A, Sharma S. Tribolayer behaviour and wear of artificially aged Al6061 hybrid composites. *Int J Automot Mech Eng.* 2021;18(2):8668-76.
36. Jayashree PK, Gowrishankar MC, Sharma S, Shetty R, Shettar M, Hiremath P. Influence of homogenization and aging on tensile strength and fracture behavior of TIG welded Al6061-SiC composites. *J Mater Res Technol.* 2020;9(3):3598-613.
37. Askeland DR, Fulay PP. *Essentials of materials science and engineering: SI edition.* Boston: Cengage Learning; 2010.